Note: An ion imaging spectrometer for studying photo-induced fragmentation in small molecules

R. Gopal, A. Sen, S. R. Sahu, A. S. Venkatachalam, M. Anand, and V. Sharma

Citation: Review of Scientific Instruments **89**, 086107 (2018); doi: 10.1063/1.5049844
View online: https://doi.org/10.1063/1.5049844
View Table of Contents: http://aip.scitation.org/toc/rsi/89/8
Published by the American Institute of Physics

REVIEW OF SCIENTIFIC INSTRUMENTS **89**, 086107 (2018)

Note: An ion imaging spectrometer for studying photo-induced fragmentation in small molecules

R. Gopal,[1] A. Sen,[2] S. R. Sahu,[3] A. S. Venkatachalam,[3] M. Anand,[1] and V. Sharma[3,a)]
[1]*Tata Institute of Fundamental Research, Hyderabad 500107, India*
[2]*Indian Institute of Science Education and Research, Pune 411008, India*
[3]*Indian Institute of Technology Hyderabad, Kandi 502285, India*

(Received 26 July 2018; accepted 2 August 2018; published online 14 August 2018)

A three-dimensional ion imaging spectrometer has been designed and calibrated by ion trajectories simulations. We present a recipe for the verification of the calibration by obtaining kinetic energy (*KE*) distribution from the recorded flight times alone and consequently correlating the two *KE* spectra. *Published by AIP Publishing.* https://doi.org/10.1063/1.5049844

We report the design of a simple ion imaging spectrometer. The spectrometer uses a single ion extraction field, lensing field, and a field-free drift region[1] coupled with a position sensitive delay line anode detector to obtain 3D imaging of the ion momenta. We used time tagged position images to extract a high resolution 2D position image. Kinetic Energy (*KE*) distributions from the 2D position image are obtained using ion trajectory simulations. In studies hitherto, the question of calibration of the obtained energies has not been addressed satisfactorily. The general consensus is to use trajectory simulations to arrive at the calibration as with Refs. 2–5, and no verification of the same is demonstrated. In certain cases,[2] particularly for electron spectrometers and using variable energy photon sources, one can verify the said calibration. In this note, in the absence of such variable energy photon sources, we show a new method to verify the calibration, using ion imaging alone and using single wavelength strong field dissociation.

The spectrometer (Fig. 1) uses three electrodes (pusher, puller, and ground plate) and a drift tube.[1] The pusher plate has a central 250 μm hole which is coupled to the gas line to form an effusive jet into the interaction region. The puller plate is placed at a distance of 22 mm from the pusher plate to form the extraction region. The acceleration region leads to a drift region terminated at the exit by a Ni-mesh with 95% optical transparency. The 170 mm drift tube has a clear aperture of 40 mm throughout. The ions from the interaction region are imaged on to a 40 mm diameter position sensitive detector. The length of the acceleration region and the drift region satisfies the Wiley-McLaren (WM) condition.[6] The focusing condition for positively charged particles was simulated using SIMION 8.0 (Scientific Instrument Services, Inc., USA). We considered a three dimensional Gaussian source of O^+ ions located on the axis at a distance of 262 mm from the detector at the central point between the pusher and puller plates. The spatial spread of the ions was taken to be 4 mm × 4 mm (FWHM) in the plane perpendicular to the spectrometer axis with 0.4 mm extension along the spectrometer axis. The initial momentum of the ions was oriented at 45° to the spectrometer axis with a thermal spread imposed on the discrete energies of the ions (1 eV, green; 2 eV, blue; 3 eV, black in Fig. 1) as the initial condition. For a voltage configuration of 645 V and 478 V on the pusher and puller plates, respectively, the focusing is shown in Fig. 1. The ideal voltage ratio (V_{puller}/V_{pusher}) is seen to be 0.74 for this geometry.

To obtain a calibration of the position on the detector to the initial energy of the ion, trajectories for multiple energies of ions, for example, O^+ ion (3×10^5 particles for each energy), were generated and the position splats and flight times recorded. In this case, the initial velocity was distributed within a 15° double cone with their axes perpendicular to the spectrometer axis. In other words, from the possible 3D velocity distribution of ions from the reaction zone, we restrict the simulation to those ions emitted in the plane perpendicular to the spectrometer axis. Experimentally, in ion imaging, this is implemented either by delayed pulse extraction[7] or more popularly by applying a time gate on the position sensitive detector.[8] Essentially, by gating the time response of the detector, from the 3D velocity sphere, a 2D slice can be chosen. We used a different implementation where no hardware gate is imposed. Rather, in the post processing of all events, we chose those within our desired time range to obtain a time slice and thereby the velocity slice. In the simulation, for the 645 V/478 V configuration shown in the lower panel of Fig. 1, the radius of the ion splat as a function of the initial energy has a near parabolic dependence. A least squares cubic fit equation represents the transformation from radius to energy for O^+ ions for this voltage condition.

The designed spectrometer was built with non-magnetic components and housed in a non-magnetic stainless steel chamber which is pumped by a 350 l/s turbomolecular pump. The ultimate vacuum achieved in the chamber is 1×10^{-8} mbar, with no gas load. With the effusive gas jet, the chamber pressure was under 1×10^{-7} mbar. The Femtopower V (Spectra-Physics, Austria) laser generates 25 fs, 1 kHz, 5 mJ pulses at 800 nm. The polarisation of the laser beam is linear and is set perpendicular to the spectrometer axis using a thin $\lambda/2$ plate. A $f = 30$ cm lens is used to focus the laser to an estimated peak intensity of 2×10^{12} W/cm^2. The ions formed in the focal volume are focused on to a 40 mm position sensitive detector comprising a set of microchannel plates (MCPs) and a delay line anode (DLA, Roentdek Handels GmbH,

a)vsharma@iith.ac.in

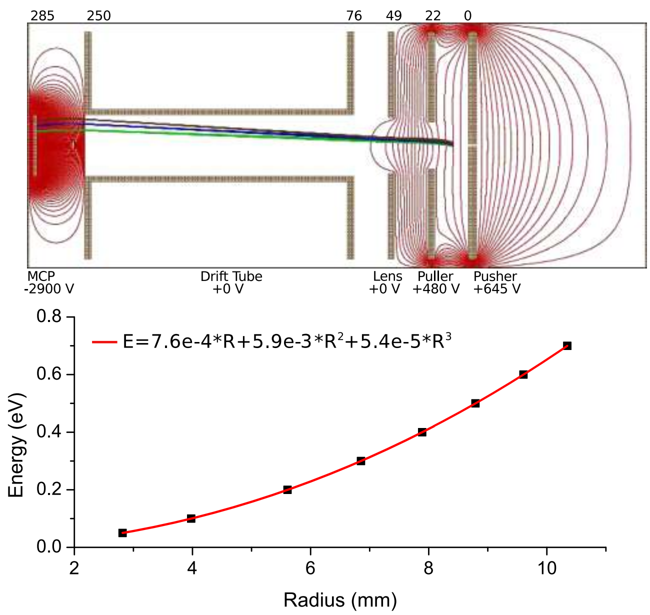

FIG. 1. Upper panel: The configuration of the spectrometer (electrodes are in brown meshes) including a SIMION based simulation of the field lines (red) in the spectrometer. Lower panel: The plot of the radius of the impacting ions on the detector as a function of the energy for the voltage setting above as simulated in SIMION.

Germany) which can encode the position (x, y) of impact of the ions on the detector. The time-of-flight (ToF, t) is calculated from the arrival time of the MCP signal relative to a fast photodiode signal from the laser. The (x, y, t) triplet of the ion splat information of each event is stored in a list mode data.

Under the assumption that the applied electric fields have no components except along the spectrometer axis, we can easily arrive at the following relations[4,9] for the initial transversal and longitudinal ion momentum ($\vec{p_r}$ and $\vec{p_z}$, respectively, in a.u., m in amu, qU in eV, distances in cm, and time in ns):

$$\vec{p_r} = 11.6 \cdot \frac{\vec{r}}{2a+d} \cdot \sqrt{qU \cdot m_{ion}}, \tag{1}$$

$$\vec{p_z} = 8.042 \times 10^{-3} \cdot \frac{qU}{a} \cdot \Delta T \hat{z}. \tag{2}$$

Here U is the acceleration potential over a distance a with respect to the reaction point, and d is the field free drift region before detection. $\vec{r}$ is the radial vector of the ion in the detector plane. ΔT is the difference between the flight times of the ion with zero longitudinal momentum t_0 and the ion hit under consideration t. In most cases, the median time of the distribution for the ion is taken as t_0. So $t < t_0$ corresponds to ions emitted initially in the direction of the detector and vice-versa for $t > t_0$. These first order equations allow us to associate the radial position and the ToF with the transverse and longitudinal momentum, respectively.

To quantify the results in terms of kinetic energy distributions of ions from the raw position and time data, we return to the above first-order equations wherein the radial and transverse motions are decoupled. These equations can directly be used to obtain the transformations from the detected position and time to momenta for spectrometers based on homogeneous fields as in Ref. 9. Here, however, the radial lens couples the two motions which must be accounted for in the accurate analytical descriptions. Semi-analytical transformations can be obtained by introducing a multiplicative "magnification"[4] or "bending"[5] factor to the transversal momenta. This coefficient is obtained from ion flight simulations in SIMION. Furthermore, arrival times are now dependent on the radial position for the marginal ion trajectories, and the modification in longitudinal ion momentum is effected by approximating a quadratic dependence of the flight time deviation on the radial position. Again the fitting parameters are easily obtained from ToF simulations in SIMION. However, we do note that the transverse homogeneity of the fields near the reaction zone has the most effect on the time deviation. In the absence of other field inhomogeneities, particularly at the interface of the detector and the drift tube, this deviation is indeed negligible, being in the order of 0.1%.[5]

In the absence of well-defined discrete high energy photon sources, an independent validation of the energy scale is not feasible. By reversing the polarities of the applied potentials, we can theoretically operate the same spectrometer in an electron imaging mode. By using high energy photon (UV-VUV) sources, the electron energy of the photoelectron from an atomic species such as Xe can be varied and energy scale verified. However, in practice, the imaging conditions for electrons and ions could vary significantly, particularly as the fields near the detector are different. We have therefore resorted to self-consistency checks to affirm the energy scale. In this procedure, we operate the spectrometer in a so-called ToF mode by rotating the polarisation of the laser field to be along the spectrometer axis.

As the ion fragmentation in intense laser fields is preferential along the polarisation axis, we have initially equal energy products flying forwards and backwards from the reaction point with respect to the detector. While the extraction field turns around the backward emitted fragments, for given ionic species, the median ToF represents fragments with zero KE. The difference in ToF with respect to the median ToF yields the KE of the ions. Processes which result in fragments with high KE such as Coulomb Explosion (CE) result in sharp peaks in the ToF spectrum, symmetric with respect to the median ToF (KE = 0) and are easily identifiable in comparison with low energy dissociative products from different quantum which appear as kinks over a continuous background.

We studied the photo-fragmentation of CH_3I in moderate intensity femtosecond laser pulses in a low field extraction (V_{pusher}/V_{puller}: 260/195), with the polarisation of the laser field parallel to the spectrometer axis. To unambiguously isolate the CE events from dissociative fragmentation, multi-hit acquisition was obtained, and a correlation plot between the first hit and the second hit was derived. Islands corresponding to coincident CH_3^+ and I^+ were identified and isolated for obtaining the ToF distribution for both CH_3^+ and I^+. To invert the ToF spectrum and thereby arrive at the KE, we have considered Eq. (2) with a multiplicative correction factor[8] to account for the inhomogeneous lens fields. To obtain this factor, we simulated two cases. In the first case, ToF difference between the same energy ions flying in the opposite direction was obtained for different KE O^+ ions with the lensing fields present (ΔT_L). Second, each electrode was capped with

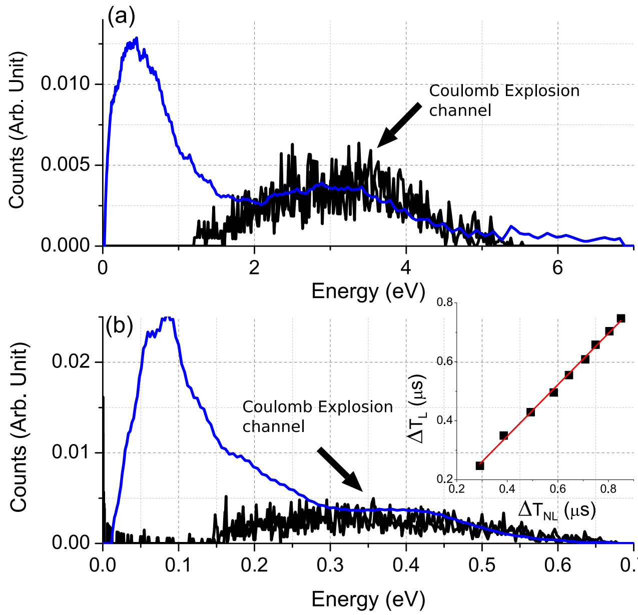

FIG. 2. (a) (Blue curve) *KE* spectrum for CH_3^+ ions obtained from the time-sliced position image. Black curve is the *KE* distribution for CH_3^+ ions obtained from the ToF spectrum. (b) (Blue curve) *KE* spectrum for I^+ ions obtained from the position image while the black curve is the *KE* distribution for I^+ ions obtained from the ToF spectrum. In the inset, the simulated time difference between the arrival times of the forward and backward emitted ions in ToF generated for various energies when the spectrometer is operated with lensing fields (ΔT_L) compared against time difference simulations for a spectrometer with homogeneous, lensless fields (ΔT_{NL}).

meshes, simulating homogeneous, lensless fields, and the same forward-backward ToF difference was obtained (ΔT_{NL}). In the inset of Fig. 2, the correlation between ΔT_{NL} and ΔT_L is plotted (black squares) and a linear fit (red) is evident. Keeping in mind that ΔT_{NL} represents the homogeneous fields for which Eq. (2) is satisfied, we use the slope of the above correlation (0.9) as the multiplicative correction factor in Eq. (2) to invert the ToF in the experiment, which is plotted as black curves in Figs. 2(a) and 2(b). Then, for the same laser conditions, but with laser polarisation being perpendicular to the spectrometer axis, the experiment was repeated in the imaging mode. The *KE* is now obtained from the time-sliced position image, as described earlier, for both CH_3^+ and I^+ which are plotted as blue curves in Figs. 2(a) and 2(b). While the full *KE* spectra contain dissociative fragmentation channels, the CE channel is indicated by arrows as the high *KE* shoulder in both spectra. The correspondence of the CE peak for *KE* spectra obtained in both methods is clear. Corrales *et al.*[10] report the total Kinetic Energy Release (*KER*) spectrum with identified CE peaks at ~4.4 eV, 5.3 eV, and 6.7 eV, in contrast to our total *KER* of ~4 eV. We note that Liu *et al.*[11] have also observed peaks with a *KER* of 4.03 eV, as expected by theoretical calculations in Ref. 10. However, unambiguous assignment and understanding any such discrepancy with the literature requires further investigation, which is currently underway.

In summary, we obtain *KE* from the time sliced 2D position images obtained from an ion imaging spectrometer. The energy calibration is through SIMION based ion trajectory simulations. The verity of the simulations is tested against *KE* spectra obtained from ToF alone. The method illustrated does not rely on existence of high energy photon sources or on calibration using electrons. We believe this will be of general importance to the atomic and molecular physics community and in particular to studies of molecular dissociation phenomena in moderate to strong laser fields.

The funding of DST/SERB (No. SB/FTP/PS-010/2014), laser facility of TIFR-H and discussions with Professor M.K. are gratefully acknowledged.

[1] A. T. J. B. Eppink and D. H. Parker, Rev. Sci. Instrum. **68**, 3477 (1997).
[2] A. Vredenborg, W. G. Roeterdink, and M. H. M. Janssen, Rev. Sci. Instrum. **79**, 063108 (2008).
[3] E. P. Månsson, S. L. Sorensen, C. L. Arnold, D. Kroon, D. Guénot, T. Fordell, F. Lépine, P. Johnsson, A. L'Huillier, and M. Gisselbrecht, Rev. Sci. Instrum. **85**, 123304 (2014).
[4] J. Laksman, D. Céolin, E. P. Månsson, S. L. Sorensen, and M. Gisselbrecht, Rev. Sci. Instrum. **84**, 123113 (2013).
[5] A. Khan, L. C. Tribedi, and D. Misra, Rev. Sci. Instrum. **86**, 043105 (2015).
[6] W. C. Wiley and I. H. McLaren, Rev. Sci. Instrum. **26**, 1150 (1955).
[7] C. R. Gebhardt, T. P. Rakitzis, P. C. Samartzis, V. Ladapoulos, and T. N. Kitsopoulos, Rev. Sci. Instrum. **72**, 3848 (2001).
[8] D. Townsend, M. P. Minitti, and A. G. Suits, Rev. Sci. Instrum. **74**, 2530 (2003).
[9] J. Ullrich, R. Moshammer, A. Dorn, R. Dorner, L. Ph. H. Schmidt, and H. Schmidt-Böcking, Rep. Prog. Phys. **66**, 1463 (2003).
[10] M. E. Corrales, G. Gitzinger, J. González-Vázquez, V. Loriot, R. de Nalda, and L. Bañares, J. Phys. Chem. A **116**, 2669 (2012).
[11] H. Liu, Z. Yang, Z. Gao, and Z. Tang, J. Chem. Phys. **126**, 044316 (2007).